Published in final edited form as:

J Thromb Haemost. 2023 April ; 21(4): 995–1009. doi:10.1016/j.jtha.2023.01.009.

Comprehensive analysis of platelet glycoprotein Ibα ectodomain glycosylation

Marie A. Hollenhorst[1,2,3], **Katherine H. Tiemeyer**[1], **Keira E. Mahoney**[4], **Kazuhiro Aoki**[5], **Mayumi Ishihara**[6], **Sarah C. Lowery**[4], **Valentina Rangel-Angarita**[4], **Carolyn R. Bertozzi**[1,7,8], **Stacy A. Malaker**[4]

[1]Sarafan ChEM-H, Stanford University, Stanford, California, USA

[2]Department of Pathology, Stanford University, Stanford, California, USA

[3]Department of Medicine, Division of Hematology, Stanford University, Stanford, California, USA

[4]Department of Chemistry, Yale University, New Haven, Connecticut, USA

[5]Department of Cell Biology, Neurobiology and Anatomy, Medical College of Wisconsin, Milwaukee, Wisconsin, USA

[6]Cancer Center, Medical College of Wisconsin, Milwaukee, Wisconsin, USA

[7]Department of Chemistry, Stanford University, Stanford, California, USA

[8]Howard Hughes Medical Institute, Stanford University, Stanford, California, USA

Abstract

Background: Platelet glycoprotein (GP) Ibα is the major ligand-binding subunit of the GPIb-IX-V complex that binds von Willebrand factor. GPIbα is heavily glycosylated, and its glycans have been proposed to play key roles in platelet clearance, von Willebrand factor binding, and as target antigens in immune thrombocytopenia syndromes. Despite its importance in platelet biology, the glycosylation profile of GPIbα is not well characterized.

Objectives: The aim of this study was to comprehensively analyze GPIbα amino acid sites of glycosylation (glycosites) and glycan structures.

Correspondence Stacy A. Malaker, Department of Chemistry, Yale University, 275 Prospect Street, New Haven, CT 06511, USA., stacy.malaker@yale.edu.

Carolyn R Bertozzi and Stacy A Malaker contributed equally to this work.

AUTHOR CONTRIBUTIONS

M.A.H., C.R.B., and S.A.M. designed the project. M.A.H., K.H.T., K.E, M., K.A., M.I., V.R.-A., S.C.L., and S.A.M. performed the experiments. M.A.H. and K.H.T. wrote the manuscript. All authors interpreted data and revised the manuscript. All authors read and approved the final paper.

DECLARATION OF COMPETING INTERESTS

M.A.H. received consulting fees from Dova Pharmaceuticals, Janssen Pharmaceuticals, and Sonder Capital. C.R.B. is a co-founder and scientific advisory board member of Lycia Therapeutics, Palleon Pharmaceuticals, Enable Bioscience, Redwood Biosciences (a subsidiary of Catalent), OliLux Bio, Grace Science LLC, and InterVenn Biosciences. S.A.M. is a consultant for InterVenn Biosciences and Arkuda Therapeutics. S.A.M. and C.R.B. are inventors on a Stanford patent related to the use of mucinases for glycoproteomic analysis. The remaining co-authors have no conflicts of interest to disclose.

Methods: GPIbα ectodomain that was recombinantly expressed or that was purified from human platelets was analyzed by Western blot, mass spectrometry glycomics, and mass spectrometry glycopeptide analysis to define glycosites and the structures of the attached glycans.

Results: We identified a diverse repertoire of N- and O-glycans, including sialoglycans, Tn antigen, T antigen, and ABO(H) blood group antigens. In the analysis of the recombinant protein, we identified 62 unique O-glycosites. In the analysis of the endogenous protein purified from platelets, we identified 48 unique O-glycosites and 1 N-glycosite. The GPIbα mucin domain is densely O-glycosylated. Glycosites are also located within the macroglycopeptide domain and mechanosensory domain.

Conclusions: This comprehensive analysis of GPIbα glycosylation lays the foundation for further studies to determine the functional and structural roles of GPIbα glycans.

Keywords

blood group antigens; glycosylation; glycomics; platelet glycoprotein GPIb-IX complex; platelet membrane glycoproteins

1 | INTRODUCTION

Adhesion of platelets to the subendothelium is a critical event in the hemostatic response to vascular injury. Platelet adhesion is mediated by an interaction between the platelet membrane glycoprotein Ibα (GPIbα) and von Willebrand factor (VWF) that is immobilized on the vessel wall [1–3]. The importance of this interaction is underscored by pathogenic GPIbα mutations that lead to bleeding in patients with Bernard-Soulier syndrome and platelet-type von Willebrand disease (VWD) [4,5]. In addition to its role in binding VWF, GPIbα regulates platelet clearance and can be a target of pathogenic antibodies in immune-mediated thrombocytopenia syndromes [6–8].

GPIbα is heavily glycosylated; glycans account for approximately 40% to 60% of the mass of the GPIbα ectodomain [9–12]. GPIbα is known to carry both of the following 2 major types of protein glycans: 1) extracellular mucin-type O-glycans and 2) N-glycans [9–12]. Mucin-type O-glycosylation is initiated by the addition of N-acetylgalactosamine (GalNAc) in α-linkage to serine (Ser) or threonine (Thr) to form the Tn antigen (GalNAcαSer/Thr) (Figure 1A, B) [13]. The addition of galactose (Gal) in β1-3 linkage to GalNAc forms the unsubstituted core 1 O-glycan (Galβ1-3GalNAcαSer/Thr), also referred to as T antigen. The unsubstituted core 2 O-glycan (GlcNAcβ1-6[Galβ1-3] GalNAcαSer/Thr) is formed by the addition of *N*-acetylglucosamine (GlcNAc) to the core 1 O-glycan. Unsubstituted core 1 and core 2 O-glycans can be extended to form a variety of complex O-glycan structures. N-glycans modify asparagine residues and can be 1 of 4 major types: paucimannose, oligomannose, hybrid, or complex (Figure 1C) [14]. O- and N-glycans can terminate with a variety of epitopes including sialic acid and the antigens that define the ABO blood groups (termed the ABH antigens) (Figure 1D).

GPIbα has been described as a mucin-domain GP [15]. These proteins are characterized by regions rich in O-glycosylated Ser/Thr residues, which cause the protein to adopt a rigid “mucin fold” where O-glycans extend out like “bottle-brush” bristles from an elongated

peptide core [16,17]. The GPIbα mucin domain is embedded within a larger region termed the macroglycopeptide domain (Figure 1E, Supplementary Figure S1 and Supplementary Table S1).[1] The O-glycans in the mucin and macroglycopeptide domains are thought to promote the projection of the N-terminal VWF ligand-binding domain (LBD) away from the platelet surface [16,17]. GPIbα is endogenously cleaved by the protease ADAM17, resulting in soluble GPIbα ectodomain, also known as glycocalicin [18].

Beyond their structural role in rigidifying the macroglycopeptide region, GPIbα glycans are likely involved in several other aspects of platelet biology. It is well-established that loss of sialic acid from platelet glycans leads to accelerated platelet clearance [6,7,19–21]. This desialylation has been suggested to cause or contribute to the development of thrombocytopenia in several disease contexts, including immune thrombocytopenia (ITP), sepsis, and influenza virus infection [7,21–23]. Although the mechanism by which desialylated platelets are cleared is the subject of controversy in the literature, most of the data point toward a central role of GPIbα glycan desialylation [6,7,19,20].

In addition to their likely role in promoting clearance of desialylated platelets, GPIbα glycans are potential antigens targeted by antiplatelet (or anti-megakaryocyte) immune responses in ITP and other immune-mediated thrombocytopenias [19–21]. In particular, immune responses against Tn and T antigens have been proposed to be important mechanisms in immune-mediated thrombocytopenia syndromes [24–26]. Recently, there has been growing interest in the possibility that platelet ABH antigens are relevant to hemostasis, and this has been proposed as a mechanism that could explain the association between ABO blood type and the risk of thrombosis or bleeding [27,28]. A final aspect of platelet biology in which glycans are likely important is in the unfolding of the GPIbα mechanosensory domain (MSD) [29]. The MSD unfolds on VWF binding and pulling, leading to conformational changes in the GPIb-IX complex that ultimately trigger intraplatelet signaling [29]. Sialylation of the MSD has also been shown to regulate MSD unfolding [29].

To date, structural characterization of GPIbα glycans has been limited. GPIbα was proposed to have approximately 60 O-glycosites based on compositional analysis of GPIbα monosaccharides and amino acids [10]. However, only 10 glycosites have been previously experimentally determined (Supplementary Table S2) [3,30–32]. Studies of purified GPIbα glycans have revealed the structures of approximately 12 glycans, including core 1 and core 2 O-glycans and complex N-glycans (Supplementary Figure S2) [11,12,33–36]. Both N- and O-glycans with terminal α(1,2)-linked fucose have been observed [34]. These structures are consistent with H antigens but were not described as such in these publications [31,33]. Antigen capture enzyme-linked immunosorbent assay and Western blot experiments have suggested that GPIbα bears A and B antigens, but the corresponding glycan structures and glycosites have not been confirmed experimentally [37–39] This knowledge gap hinders our ability to understand the roles of GPIbα glycans in health and disease.

[1]GPIbα amino acids are numbered throughout the manuscript according to UniprotKB –P07359.2 (GP1BA_HUMAN). The GPIbα gene is polymorphic; it codes for GPIbα protein with a variable number (1–4) of tandem 13-amino acid repeats (SEPAPSPTTPEPT). This sequence has 3 tandem repeats. See Figure S1 for more details regarding the amino acid sequence.

It is not surprising that our knowledge of GPIbα glycosylation is incomplete, as mucin-domain GPs are notoriously challenging to study [40]. This is partially because of their resistance to cleavage by standard proteases used to generate glycopeptides for mass spectrometry (MS) analysis [40]. To address this challenge, we previously characterized secreted protease of C1 esterase inhibitor (StcE), an enzyme that cleaves mucins (ie, a mucinase) into glycopeptides amenable to MS analysis [40]. We demonstrated that StcE proteolyzed GPIbα, suggesting that a mucinase digestion strategy may be effective in facilitating its analysis by a targeted protein glycoproteomic approach [40].

In this study, we undertook a detailed analysis of human GPIbα glycosylation. We purified the GPIbα ectodomain from human platelets and then used a combination of experimental strategies, including mucinase digestion methods, to carry out a glycomics-informed MS glycopeptide analysis [41,42]. By integrating information from glycomics and glycopeptide analysis, we defined glycan structures in detail and site-localized them to specific amino acids.

2 | MATERIALS AND METHODS

2.1 | Materials

Recombinant GPIbα was obtained from R&D Systems; the gene coding for the human GPIbα ectodomain was overexpressed in an NS0-derived mouse myeloma cell line. Apheresis platelets of blood type A, B, or O were purchased as research products from Bloodworks Northwest (Supplementary Table S3). Platelets were stored at room temperature with gentle agitation and were used up to 7 days past their transfusion outdated. Further details are available in the Supplementary material.

2.2 | Purification of GPIbα ectodomain from human platelets

The soluble ectodomain of GPIbα (glycocalicin) was purified from apheresis platelets using an adaptation of previously reported protocols [43,44]. Three to 5 units of apheresis platelets, generally from distinct donors, were pooled for each purification, so GPIbα in each preparation came from up to 5 different individuals. Platelets were washed with ice-cold PBS. Platelet suspensions were sonicated and then incubated at 37 °C for 1 hour. After incubation, platelet suspensions were centrifuged and the supernatant was purified by wheat germ agglutinin agarose gravity column followed by anion exchange chromatography using a HiTrap DEAE-FF 1 mL column (Cytiva) on an AKTA pure liquid chromatography (LC) system (Cytiva). Further details are available in the Supplementary material.

2.3 | Western blot analysis of GPIbα

Purified GPIbα was separated by sodium dodecyl sulfate-polyacrylamide gel electrophoresis and then transferred to a nitrocellulose membrane. The following primary antibodies were used: anti-A or anti-B murine monoclonal blend (1:10; Ortho-Clinical Diagnostics), rabbit monoclonal anti-GPIbα (1:10,000; Abcam ab 210407, EPR19204). Blots were incubated with the following secondary antibodies for 1 hour at room temperature: IRDye 800 CW goat anti-mouse IgM (Li-COR, 1:15,000), IRDye 800 CW goat anti-rabbit (Li-COR, 1:15,000). Blots were imaged on the Odyssey DLx imaging system (Li-COR).

H antigen was visualized using biotinylated *Ulex europaeus* I (Vector Laboratories). A room temperature incubation was performed for the secondary antibody (IRDye 800 CW Streptavidin, 1:1000 in Carbo-Free blocking buffer containing 0.2% Tween-20). Sialic acid-containing GPIbα glycans were also assessed by lectin blotting using the *Sambucus nigra* (SNA/EBL) biotinylated lectin (Vector Laboratories) at 2 μg/μL. Further details are available in the Supplementary material.

2.4 | Release of glycans from purified platelet-derived human GPIbα ectodomain for glycomics analysis

Glycan release was performed according to previously reported methods [41,45–48]. Purified human platelet GPIbα ectodomain was digested with trypsin. Tryptic peptides were purified and then treated with peptide-N-glycosidase F (Promega) to release N-glycans. Released N-glycans were purified by a Sep-Pak C18 cartridge column. O-glycans were released from N-glycan-free GPIbα glycopeptides by reductive β-elimination. Further details are available in the Supplementary material.

2.5 | MS glycomics analysis

Released N- and O-glycans were analyzed as their permethylated forms by nanospray ionization MS in positive mode [41,45–48]. Permethylated glycans were dissolved in 50 μL of 1 mM sodium hydroxide in methanol/water (1:1) for infusion into an Orbitrap linear ion trap mass spectrometer (Orbitrap-LTQ; Thermo Fisher Scientific) using a nanospray source at a syringe flow rate of 0.80 μL/min and capillary temperature of 210 °C. For fragmentation by collision-induced dissociation in tandem MS (MS/MS) and MS^n, a normalized collision energy of 35% to 40% was used. MS data were manually annotated using the Xcalibur software package version 2.0 (Thermo Fisher Scientific) as previously described [41,49–51]. Glycans were also analyzed by total ion mapping to detect minor glycan components. Graphic representations of *N*-glycan monosaccharide residues were consistent with the Symbol Nomenclature for Glycans as adopted by the glycomics and glycobiology communities [52,53]. Glycomics data and metadata were obtained and presented in accordance with MIRAGE standards and the Athens Guidelines [54]. All raw MS data were deposited at GlycoPost, accession #GPST000275 [55]. Further details are available in the Supplementary material.

2.6 | *In vitro* digestion of GPIbα ectodomain for MS glycopeptide analysis

The ectodomain of GPIbα was digested with several different conditions to maximize protein coverage and glycopeptide identification. When proteases were included in the digestion, peptides were subsequently reduced in 2 mM dithiothreitol at 65 °C for 30 minutes. After cooling, iodoacetamide was added to a concentration of 3 mM and allowed to react for 15 minutes in the dark at room temperature. Samples were then diluted using 50 μL of 50 mM ammonium bicarbonate. All digests were performed in ammonium bicarbonate, pH 7.5. Mucinase digests (eg, StcE and SmE) were performed overnight and protease digests (eg, GluC and trypsin) were performed the following day for 6 hours. In cases where N-glycans were removed, PNGaseF (NEB) was diluted 1:10 and 1 μL was added to the mucinase digests (20–60 μL) overnight. In sialidase-treated samples (recombinant protein only), 1 μL of sialoEXO (Genovis) was added to 39 μL of water, then 1 μL of the

dilution was added to the reaction. All digests were incubated at 37 °C. The combinations of proteases used and their enzyme: substrate ratios were as follows: SmE/GluC (1:20, 1:100), SmE/trypsin (1:20, 1:100), StcE/GluC (1:20, 1:100), StcE/Thermolysin (1:20, 1:100), SmE only (1:20), and ImpA only (1:20). Reactions were quenched using 100 μL of 0.5% formic acid in ultrapure water (Pierce). C18 clean-up was performed using 1 mL strataX columns (Phenomenex). Each column was hydrated with 1 mL of acetonitrile, followed by a 1 mL rinse of 0.1% formic acid in water ("buffer A"). The samples were then added to the column and rinsed with 150 μL of 0.1% formic acid. The samples were eluted twice with 150 μL of 0.1% formic acid in 30% acetonitrile and dried by vacuum centrifugation. Finally, a hydrophilic interaction chromatography clean-up was performed to remove polyethylene glycol contamination. The samples were reconstituted in 10 μL of buffer A for MS analysis. Further details are available in the Supplementary material.

2.7 | Glycopeptide MS data acquisition and analysis

Samples were analyzed by online nanoflow LC-MS/MS using an Orbitrap Eclipse Tribrid mass spectrometer (Thermo Fisher Scientific) coupled to a Dionex Ultimate 3000 HPLC (Thermo Fisher Scientific). Higher-energy collisional dissociation, electron transfer dissociation, and electron transfer dissociation with supplemental activation were performed. Raw files were searched using O-Pair search with MetaMorpheus and Byonic (ProteinMetrics) against a database containing the protein of interest [56,57]. Files were searched with various cleavage specificities dependent on digestion conditions and the search algorithm used. For O-Pair, an O-glycan database was built based on the glycomics data generated in this study, and the maximum number of glycosites per peptide was set to 4. For Byonic, the O-glycan common 9 database was used with a common max of 3. Peptide hits were filtered using a 1% FDR and, in O-Pair, a q-value of <0.01. All peptides were manually validated and/or sequenced using Xcalibur software (Thermo Fisher Scientific). Candidate sequences were obtained from search algorithms and an in-house program was used to identify MS2 spectra containing oxonium ions and the associated naked peptide backbone. Higher-energy collisional dissociation spectra were used to assign naked peptide sequences, glycan compositions, and characteristic fragmentation patterns. Electron transfer dissociation and/or electron transfer dissociation with supplemental activation were then used to localize glycosites. The MS proteomics data have been deposited to the ProteomeXchange Consortium via the PRIDE partner repository with the dataset identifier PXD035030 [58,59]. Further details are available in the Supplementary material.

3 | RESULTS

3.1 | Western blot analysis of human platelet-derived GPIbα ectodomain confirms presence of ABH antigens

Given our interest in the potential hemostatic relevance of GPIbα ABH antigens, we first aimed to validate prior reports that this protein bears ABH antigens. We purified the GPIbα ectodomain (glycocalicin) from human apheresis platelets of blood type A, B, or O (Figure 2A, Supplementary Figure S3 and S4, Supplementary Table S4), and subjected the purified protein to Western blot analysis with anti-A or anti-B antibodies (Figure 2D).

Type A GPIbα, but not B or O, showed reactivity with anti-A antibody, and this reactivity was abolished when the protein was treated with a recombinant α-*N*-acetylgalactosaminidase that cleaves the terminal GalNAc residue found in the A antigen (Figure 2B, D). Similarly, type B GPIbα, but not A or O, showed reactivity on Western blot with anti-B antibody, and this reactivity was abolished with recombinant α-galactosidase treatment which cleaves the terminal Gal residue found in the B antigen (Figure 2C, D).

To test for H antigen, we performed lectin blot analysis using *Ulex europaeus* (UEA-I) lectin. UEA-I lectin binds fucose-containing glycans and is selective for the H antigen over A or B. GPIbα from type A, B, and O platelets showed reactivity on the UEA-I lectin blot (Figure 3). Individuals with non-O blood types are known to express H antigen, so UEA-I reactivity on the protein from type A and B platelets was not surprising [39,60]. As expected, no UEA-I reactivity was seen following fucosidase treatment. As further validation of the presence of the H antigen on GPIbα from type O platelets, type O GPIbα was treated with recombinant human ABO glycosyltransferase type B. This led to a band that showed reactivity on an anti-B Western blot (Supplementary Figure S5). Enzymatic removal of *N*-glycans from A or B GPIbα with PNGaseF did not substantially diminish the A or B signal on Western blot, suggesting that ABH antigens do not reside exclusively on *N*-glycans (Supplementary Figure S6–S8).

3.2 | Quantification of human platelet-derived GPIbα ectodomain monosaccharides confirms extensive glycosylation

We next sought to confirm that GPIbα is heavily glycosylated and to quantify monosaccharides of interest. We were particularly interested in determining the abundance of 1) sialic acid and 2) fucose, which is a constituent of ABH antigens. Purified GPIbα ectodomain from blood type O human apheresis platelets was treated with acid to hydrolyze the glycans into monosaccharides. The monosaccharides were quantified by established LC methods (Supplementary Table S5 and S6). The most common type of sialic acid in humans is *N*-acetylneuraminic acid (Neu5Ac). This analysis revealed the following molar ratios of monosaccharide to protein (mean ± SD): Neu5Ac 58.6 ± 0.1, Gal 56.5 ± 3.2, GlcNAc 33.2 ± 0.7, GalNAc 21.1 ± 0.6, mannose 6.7 ± 0.1, Fuc 5.1 ± 0.2, and glucose 2.0 ± 0.3 (Supplementary Figure S9 and S10, Supplementary Table S7).

3.3 | MS glycomics analysis of human platelet-derived GPIbα ectodomain reveals a diverse repertoire of N- and O-glycans

After validating that GPIbα carries ABH antigens and sialic acid, we aimed to determine what glycans bear these moieties by MS glycomics analysis. Purified GPIbα ectodomain from blood type A, B, or O human apheresis platelets were subjected to trypsin digestion and PNGaseF treatment to release N-glycans. The N-glycans were saved and de-N-glycosylated glycopeptides were subjected to β-elimination to release O-glycans. Separately, N- and O-glycans were permethylated and analyzed by MS. The glycan sequences for certain isobaric structures were determined by MS^n fragmentation. We did not in all cases perform complete MS^n analysis to allow unambiguous differentiation between isobaric glycans. We graphically represented glycans according to the most likely structure(s) based on our MS data and knowledge of previously reported glycan structures and biosynthetic

pathways. However, we did not always have complete information to unambiguously assign the monosaccharide linkages, and some of the detected N-glycan masses likely represent mixtures of isobaric structures. The true N-glycan structures may differ in the number of branches compared with what we have depicted here. Additionally, the angle at which branching monosaccharide residues are depicted is not meant to imply specific linkage positions or anomeric configuration.

Eight distinct O-glycans were identified that were >3% relative abundance on the full MS profile (Figure 4 and Supplementary Figure S11). The most abundant O-glycan in each sample was a disialylated core 2 hexasaccharide (*m*/*z* 864.4 and 1705.8); which accounted for approximately 30% to 50% of the total O-glycan ion current in each sample. Most of the other observed O-glycans were core 1 or core 2 type O-glycans with variable monosaccharide extensions. Seven of the O-glycans were sialoglycans, carrying 1 to 3 sialic acid monomers per glycan. Tn and T antigens were not able to be accurately detected or quantified by glycomics given their low masses.

A terminally fucosylated complex core 2 O-glycan (*m*/*z* 770.9 and 1518.8) was detected in samples from blood types A, B, and O. The relative abundance was approximately 5% in the type O sample. MS^n analysis of this glycan confirmed the sequence as expected for the H antigen (Figure 5). The MS^3 fragment ions for the putative H antigen glycans were those expected based on the fragmentation of an H antigen standard; these were distinct from fragment ions seen with a Lewis antigen standard (Supplementary Figure S12). Three other O-glycans were found to bear the H antigen. These were <3% relative abundance in the full MS spectrum and were identified by total ion mapping analysis and confirmed by MS^n (Supplementary Figure S13). These low-abundance H-antigen O-glycans include structures where the H-antigen is a terminal modification of complex core 2 O-glycans as well as mucin type H antigen, where the H antigen is a direct modification of Ser/Thr (Figure 1D).

In an analysis of type A GPIbα, 2 O-glycans bearing A antigen epitopes were detectable in the intact MS profile; however, the signal was minimal and these glycans were not confirmed by MS^n. The B antigen was observed on 3 O-glycans in the analysis of type B GPIbα and could be confirmed by MS^n analysis (Supplementary Figure S13 and S14). H antigen was also observed on O-glycans from GPIbα from type A and B platelets, consistent with the positive signal seen on UEA-I lectin blots for GPIbα of all blood types.

Eighteen distinct N-glycan masses were identified that were >3% relative abundance in the full MS profile (Figure 6 and Supplementary Figure S15). The most abundant N-glycans in each sample were complex biantennary disialylated glycans (m/z 2792.5 and 2966.5). All identified N-glycans were of the complex type except for 1 oligomannose N-glycan (*m*/*z* 1579.8). The complex N-glycans had up to 4 antennae. Seventeen distinct N-glycans were identified that contain sialic acid, and there were up to 4 sialic acid monomers per glycan.

N-glycomics analysis of blood type O GPIbα revealed 10 N-glycans with masses compatible with an H antigen epitope, which was confirmed by MS^n fragmentation (Supplementary Figures S16 and S17). The A antigen was detected on 2 N-glycans from type A GPIbα and was confirmed by MS^n analysis (Supplementary Figure S17 and S18).

No B antigen was detected on N-glycans released from type B GPIbα. H antigen was also observed on *N*-glycans from GPIbα from type A and B platelets (Supplementary Figure S17).

3.4 | Bioinformatic analysis of GPIbα ectodomain predicts 62 glycosites

Next, we turned our attention to the identification of glycosites. N-glycosites are predicted by the consensus amino acid motif for N-glycosylation: N-X-S/T, where X can be any amino acid except proline [61]. Analysis of the GPIbα ectodomain amino acid sequence revealed 4 putative N-glycosites, including 2 in the VWF LBD (N37, N175) and one in the mucin domain (N398) (Supplementary Table S2) [61]. Conversely, there is no consensus motif for O-glycosylation. The NetOGlyc 4.0 server produces neural network predictions of O-glycosites based on previously characterized O-glycoproteins [62]. NetOGlyc 4.0 predicted 58 GPIbα O-glycosites, including 2 in the VWF LBD (T256 and S257) and 25 in the mucin domain (Supplementary Table S2).

3.5 | MS analysis of recombinant and platelet-derived GPIbα ectodomain glycopeptides

Having established the identity of the predicted glycosites, we next aimed to map GPIbα glycosites experimentally using targeted glycopeptide analysis. We first studied recombinant human GPIbα ectodomain by subjecting GPIbα to digestion with various combinations of bacterial mucinases (StcE and SmE), glycosidases, and commercially available proteases. We analyzed O-glycosites and O-glycans from the resultant glycopeptides by LC-MS/MS. We identified 62 unique O-glycosites in the recombinant protein, including 16 O-glycosites in the mucin domain (Figures 7 and 8, Supplementary Figure S19, and Supplementary Table S2). One or more O-glycan masses were identified at each of the glycosites (Supplementary Table S8).

We used similar methods to perform a glycopeptide analysis of GPIbα ectodomain purified from human platelets, this time seeking to characterize both O- and N-glycosites. We identified 48 unique O-glycosites and 1 N-glycosite in the platelet-derived protein, including 21 unique O-glycosites within the mucin domain. GPIbα from biological samples has variable numbers of tandem repeats (1–4). If we consider GPIbα with 3 tandem repeats (as in the standard Uniprot sequence), and we assume that each repeat has the same glycosites, then there would be a total of 60 glycosites in the ectodomain and 32 in the mucin domain. In the VWF LBD, we identified 1 N-glycosite (N37).

The Tn antigen was identified at 14 glycosites and the T antigen at 19 glycosites (Supplementary Table S2). With knowledge of the structures of the sialic acid and ABH antigen-bearing glycans from the glycomics analysis, we used the glycopeptide data to site-localize these glycans. We identified 38 O-glycosites that bear sialoglycans and 15 O-glycosites that bear ABH antigens (Figure 7 and Supplementary Table S2).

4 | DISCUSSION

Here, we report the most detailed analysis of platelet GPIbα glycosylation to date; we have experimentally determined 49 unique glycosites and 26 major glycan structures by MS.

Our monosaccharide analysis validates prior reports which suggested that GPIbα is heavily glycosylated [9–12]. Our data confirm that the platelet-derived GPIbα ectodomain carries abundant sialic acid, with a monosaccharide to protein molar ratio of 59 for Neu5Ac. The approximately 2:2:1:1 ratio of Neu5Ac:Gal:GalNAc:GlcNAc is consistent with monosaccharide analyses performed in some of the earliest biochemical characterizations of the GPIbα ectodomain [9]. Furthermore, the monosaccharide analysis provides insight into the relative ratios of N- vs O-glycans. Each N-glycan typically contains at least 3 Man units, while Man is characteristically absent from mucin-type O-glycans [63]. Therefore, the monosaccharide to protein molar ratio of 59 for Neu5Ac, 57 for Gal, and only 7 for Man is consistent with a preponderance of O-glycans compared with N-glycans. Finally, the detection of Fuc supports the presence of fucose-containing glycans, of which ABH antigens are 1 subtype.

Of the 4 potential GPIbα N-glycosites, 2 have been previously reported to be occupied by N-glycans (N37, N175) [30,32]. We confirmed occupancy at N37. We did not detect N-glycosylation at any other predicted N-glycosites. Of the 58 bioinformatically predicted GPIbα O-glycosites, 8 have been previously experimentally determined to be occupied by O-glycans [30,31]. In our analysis of the protein purified from platelets, we reconfirmed occupancy at 7 out of 8 of these glycosites; we did not observe O-glycosylation at the previously determined S470. Two VWF LBD O-glycosites were predicted bioinformatically (S256 and S257); these were observed to be glycosylated in our analysis of the recombinant protein but not the platelet-derived protein. As anticipated from prior work and bioinformatic analysis of the amino acid sequence, our glycoproteomic analysis revealed that the GPIbα mucin domain is densely O-glycosylated. We identified 21 O-glycosites in the GPIbα mucin domain. O-glycosites were also found in the broader macroglycopeptide domain and MSD.

Given the critical role of sialic acid in regulating platelet clearance, it is notable that 1) sialic acid (Neu5Ac) was the most abundant monosaccharide in the platelet-derived GPIbα compositional analysis, 2) we detected 24 abundant glycans that terminated in sialic acid, and 3) we identified 39 glycosites that were occupied by sialoglycans. The mechanism by which desialylated platelets are cleared remains incompletely understood. Some studies have suggested that the mechanism involves exposure of GPIbα Gal residues, followed by platelet uptake via interactions with hepatic and/or Kupffer cell asialoglycoprotein receptors [64]. Recent reports point toward a role in the desialylation of GPIbα O-glycans [7]. Our site-localization of GPIbα sialoglycans provides a map of potential glycans that could be relevant in mediating platelet clearance.

Numerous epidemiologic studies have demonstrated that risk of bleeding and thrombosis is associated with ABO blood type [28,65–68]. Blood type O individuals are at a higher risk of bleeding and a lower risk of thrombosis compared with non-O individuals. Lower levels of VWF and factor VIII (FVIII) in blood type O compared with non-O individuals are likely important drivers of this association [69]. However, 2 recent studies have led to the consideration that there may be a platelet-intrinsic mechanism that also underlies this association [28,68]. First, in a genome-wide association study, the *ABO* locus was found to be the main determinant of primary hemostasis as measured by Platelet Function

Analyzer-100 closure times [70]. The influence of ABO blood type on Platelet Function Analyzer-100 measurements was only partially explained by VWF and FVIII levels, suggesting that other mechanisms may be important [70]. Second, in a microfluidics assay, non-O platelets were found to have superior binding characteristics to VWF compared with type O platelets [27]. For the first time, we have definitively demonstrated the presence of ABH antigens on GPIbα glycans by robust Western blot assay and MS. We identified 15 glycosites that bear ABH antigen-containing glycans, largely located in the mucin domain and MSD. Whether GPIbα ABH antigen glycans affect the structure and/or function of this protein, potentially leading to changes in VWF binding, remains to be tested in future work.

Deletion of a stretch of 9 amino acids in the MSD (462–470; PTILVSATS) causes inherited platelet-type VWD [71]. We confirmed glycosylation of the protein from platelets at 3 glycosites within this sequence (T463, S467, and T469) and identified ABH antigen glycans at 2 of these sites (T463 and T469). A fourth glycosite within this stretch, S470, has been previously characterized [31]. Further studies are required to determine the relevance of glycosylation at these 4 glycosites to VWD.

The Tn and T antigens are biosynthetic precursors to more fully elaborated O-glycan structures. We identified these immature O-glycans commonly in more densely O-glycosylated stretches of GPIbα. For example, the mucin glycosites T385, T387, and T388 carried only Tn, T, or GalNAc-GalNAc, and not more mature O-glycans. This preponderance of immature O-glycan structures in densely glycosylated regions has been observed in the analysis of other proteins and may relate to steric hindrance of glycosyltransferase activity in nascent, heavily O-glycosylated proteins [72].

Antiplatelet GP antibodies lead to accelerated platelet clearance in several immune-mediated thrombocytopenia syndromes: ITP, fetal-neonatal alloimmune thrombocytopenia, posttransfusion purpura, and the Tn syndrome [8,24,26,73,74]. Prior work suggests that these antibodies may bind to platelets in a glycan-dependent manner [24,26,74]. For example, in a recent study, anti-T antigen antibodies were identified in sera from a cohort of pediatric patients with ITP and implicated in the pathogenesis of ITP [24]. Thrombocytopenia can develop in the Tn syndrome when anti-Tn antibodies bind to platelets. We have now established that GPIbα carries T and Tn antigen epitopes. This opens the door to investigation into the relevance of auto-antibodies directed against GPIbα T or Tn antigen in the pathogenesis of immune-mediated thrombocytopenia syndromes. More broadly, our characterization of GPIbα glycosylation provides insight into possible glycoepitopes that may be targeted by anti-glycan and/or anti-GPIb allo- or auto-antibodies in immune-mediated thrombocytopenia syndromes.

Some limitations of our work should be noted. We studied the glycosylation of GPIbα ectodomain that was cleaved from the surface of human platelets. The glycosylation of the cleaved ectodomain may not be the same as the glycosylation of the intact protein on the platelet surface. O-glycosylation is known to regulate the proteolytic cleavage of many proteins, so certain glycoforms of GPIbα could be preferentially proteolyzed by ADAM17 [75]. Furthermore, we purified the protein using lectin and anion exchange chromatography; these purification steps could have selectively enriched particular glycoforms. Although

our analysis has revealed many more glycosites and glycans than had previously been characterized, we may not have identified all the glycosites and glycans for 3 major reasons: 1) dense and heterogeneous glycosylation may render any individual glycopeptide too low abundance to detect and/or might hinder ionization of the glycopeptide, 2) we did not search for glycopeptide masses compatible with glycosylation and other posttranslational modifications to the same peptide, so we may not have detected glycosites located near non-glycan modifications, 3) our N-glycomics method did not detect N-glycans with m/z <1500, so we may have missed truncated N-glycans. Additionally, our analysis was limited in that it does not provide information regarding the types of glycosidic linkages between monosaccharides, for example, α(2,6) vs α(2,3)-linked sialic acid. While we performed glycomics analysis on preparations of GPIbα that were pure enough to yield a single band on Coomassie-stained sodium dodecyl sulfate-polyacrylamide gel electrophoresis, it is possible that some of the glycans observed by MS glycomics came from contaminating proteins.

5 | CONCLUSION

In summary, we report a comprehensive analysis of GPIbα glycosylation. We used MS glycomics and glycopeptide analysis to perform a site-specific analysis of GPIbα purified from human platelets. We determined 48 O-glycosites and 1 N-glycosite. We determined that GPIbα carries diverse N- and O-glycans, including sialoglycans, Tn antigen, T antigen, and ABO(H) antigens. This information lays the foundation for further studies to determine the functional and structural implications of GPIbα glycosylation in hemostasis, platelet clearance, and the antiplatelet immune response.

Supplementary Material

Refer to Web version on PubMed Central for supplementary material.

ACKNOWLEDGMENTS

Monosaccharide analysis was performed by the UC San Diego GlycoAnalytics Core. This work was supported by a Sarafan ChEM-H Physician-Scientist fellowship (to M.A.H.), the Stanford Maternal & Child Health Research Institute Instructor K Award Support Program (to M.A.H.), a National Blood Foundation Early Career Scientific Research Grant (to M.A.H.), an NIH NHBLI Pathway to Independence award (1K99HL156029-01 to M.A.H.), and NIH grant R01CA200423 (to C.R.B.). K.A. was supported by the GaLSIC collaborative research fund, at Soka University, Japan. SAM is supported by the Yale Science Development Fund, the Yale SEAS/Science Program to Advance Research Collaboration (SPARC), and National Institute of General Medical Studies R35-GM147039. K.E.M. is supported by a Yale Endowed Postdoctoral Fellowship and S.C.L. is supported by the National Institutes of Health Chemical Biology Training Grant (T32 GM067543). Some figures were created with BioRender.com.

Funding information

This work was supported by a Sarafan ChEM-H Physician-Scientist fellowship (to M.A.H.), the Stanford Maternal & Child Health Research Institute Instructor K Award Support Program (to M.A.H.), a National Blood Foundation Early Career Scientific Research Grant (to M.A.H.), an NIH NHBLI Pathway to Independence award (1K99HL156029-01 to M.A.H.), and NIH grant R01CA200423 (to C.R.B.). K.A. was supported by the GaLSIC collaborative research fund, at Soka University, Japan. SAM is supported by the Yale Science Development Fund, the Yale SEAS/Science Program to Advance Research Collaboration (SPARC), and National Institute of General Medical Studies R35-GM147039. K.E.M. is supported by a Yale Endowed Postdoctoral Fellowship and S.C.L. is supported by the National Institutes of Health Chemical Biology Training Grant (T32 GM067543).

REFERENCES

[1]. Li CQ, Dong JF, López JA. The mucin-like macroglycopeptide region of glycoprotein Ibalpha is required for cell adhesion to immobilized von Willebrand factor (VWF) under flow but not for static VWF binding. Thromb Haemost. 2002;88:673–7. [PubMed: 12362242]

[2]. Li R, Emsley J. The organizing principle of the platelet glycoprotein Ib-IX-V complex. J Thromb Haemost. 2013;11:605–14. [PubMed: 23336709]

[3]. Lopez JA, Chung DW, Fujikawa K, Hagen FS, Papayannopoulou T, Roth GJ. Cloning of the alpha chain of human platelet glycoprotein Ib: a transmembrane protein with homology to leucine-rich alpha 2-glycoprotein. Proc Natl Acad Sci U S A. 1987;84:5615–9. [PubMed: 3303030]

[4]. López JA, Andrews RK, Afshar-Kharghan V, Berndt MC. Bernard-Soulier syndrome. Blood. 1998;91:4397–418. [PubMed: 9616133]

[5]. Nurden AT, Nurden P. Inherited thrombocytopenias: history, advances and perspectives. Haematologica. 2020;105:2004–19. [PubMed: 32527953]

[6]. Jansen AJ, Josefsson EC, Rumjantseva V, Liu QP, Falet H, Bergmeier W, Cifuni SM, Sackstein R, von Andrian UH, Wagner DD, Hartwig JH, Hoffmeister KM. Desialylation accelerates platelet clearance after refrigeration and initiates GPIbα metalloproteinase-mediated cleavage in mice. Blood. 2012;119:1263–73. [PubMed: 22101895]

[7]. Wang Y, Chen W, Zhang W, Lee-Sundlov MM, Casari C, Berndt MC, Lanza F, Bergmeier W, Hoffmeister KM, Zhang XF, Li R. Desialylation of O-glycans on glycoprotein Ibα drives receptor signaling and platelet clearance. Haematologica. 2021;106:220–9. [PubMed: 31974202]

[8]. Al-Samkari H, Rosovsky RP, Karp Leaf RS, Smith DB, Goodarzi K, Fogerty AE, Sykes DB, Kuter DJ. A modern reassessment of glycoprotein-specific direct platelet autoantibody testing in immune thrombocytopenia. Blood Adv. 2020;4:9–18. [PubMed: 31891657]

[9]. Okumura I, Lombart C, Jamieson GA. Platelet glycocalicin. II. Purification and characterization. J Biol Chem. 1976;251:5950–5. [PubMed: 823155]

[10]. Judson PA, Anstee DJ, Clamp JR. Isolation and characterization of the major oligosaccharide of human platelet membrane glycoprotein GPIb. Biochem J. 1982;205:81–90. [PubMed: 6215034]

[11]. Tsuji T, Tsunehisa S, Watanabe Y, Yamamoto K, Tohyama H, Osawa T. The carbohydrate moiety of human platelet glycocalicin. J Biol Chem. 1983;258:6335–9. [PubMed: 6406478]

[12]. Korrel SA, Clemetson KJ, Van Halbeek H, Kamerling JP, Sixma JJ, Vliegenthart JF. Structural studies on the O-linked carbohydrate chains of human platelet glycocalicin. Eur J Biochem. 1984;140:571–6. [PubMed: 6327299]

[13]. Varki A, Cummings RD, Esko JD, Stanley P, Hart GW, Aebi M, Mohnen D, Kinoshita T, Packer NH, Prestegard JH, Schnaar RL, Seeberger PH. Essentials of glycobiology. In: Cold Spring Harbor. 4th edn. Cold Spring Harbor Laboratory Press; 2022.

[14]. Bagdonaite I, Malaker SA, Polasky DA, Riley NM, Schjoldager K, Vakhrushev SY, Halim A, Aoki-Kinoshita KF, Nesvizhskii AI, Bertozzi CR, Wandall HH, Parker BL, Thaysen-Andersen M, Scott NE. Glycoproteomics. Nat Rev Methods Prim. 2022;2:1–29.

[15]. Malaker SA, Riley NM, Shon DJ, Pedram K, Krishnan V, Dorigo O, Bertozzi CR. Revealing the human mucinome. Nat Commun. 2022;13:3542. [PubMed: 35725833]

[16]. Rangel-Angarita V, Malaker SA. Mucinomics as the next frontier of mass spectrometry. ACS Chem Biol. 2021;16:1866–83. [PubMed: 34319686]

[17]. Fox JE, Aggerbeck LP, Berndt MC. Structure of the glycoprotein Ib.IX complex from platelet membranes. J Biol Chem. 1988;263:4882–90. [PubMed: 3280570]

[18]. Gardiner EE, Karunakaran D, Shen Y, Arthur JF, Andrews RK, Berndt MC. Controlled shedding of platelet glycoprotein (GP)VI and GPIb-IX-V by ADAM family metalloproteinases. J Thromb Haemost. 2007;5:1530–7. [PubMed: 17445093]

[19]. Rumjantseva V, Grewal PK, Wandall HH, Josefsson EC, Sørensen AL, Larson G, Marth JD, Hartwig JH, Hoffmeister KM. Dual roles for hepatic lectin receptors in the clearance of chilled platelets. Nat Med. 2009;15:1273–80. [PubMed: 19783995]

[20]. Sørensen AL, Rumjantseva V, Nayeb-Hashemi S, Clausen H, Hartwig JH, Wandall HH, Hoffmeister KM. Role of sialic acid for platelet life span: exposure of beta-galactose results

in the rapid clearance of platelets from the circulation by asialoglycoprotein receptor-expressing liver macrophages and hepatocytes. Blood. 2009;114:1645–54. [PubMed: 19520807]

[21]. Li J, van der Wal DE, Zhu G, Xu M, Yougbare I, Ma L, Vadasz B, Carrim N, Grozovsky R, Ruan M, Zhu L, Zeng Q, Tao L, Zhai ZM, Peng J, Hou M, Leytin V, Freedman J, Hoffmeister KM, Ni H. Desialylation is a mechanism of Fc-independent platelet clearance and a therapeutic target in immune thrombocytopenia. Nat Commun. 2015;6:7737. [PubMed: 26185093]

[22]. Grewal PK, Aziz PV, Uchiyama S, Rubio GR, Lardone RD, Le D, Varki NM, Nizet V, Marth JD. Inducing host protection in pneumococcal sepsis by preactivation of the Ashwell-Morell receptor. Proc Natl Acad Sci U S A. 2013;110:20218–23. [PubMed: 24284176]

[23]. Jansen AJG, Spaan T, Low HZ, Di Iorio D, van den Brand J, Tieke M, Barendrecht A, Rohn K, van Amerongen G, Stittelaar K, Baumgärtner W, Osterhaus A, Kuiken T, Boons GJ, Huskens J, Boes M, Maas C, van der Vries E. Influenza-induced thrombocytopenia is dependent on the subtype and sialoglycan receptor and increases with virus pathogenicity. Blood Adv. 2020;4:2967–78. [PubMed: 32609845]

[24]. Lee-Sundlov MM, Burns RT, Kim TO, Grozovsky R, Giannini S, Rivadeneyra L, Zheng Y, Glabere SH, Kahr WHA, Abdi R, Despotovic JM, Wang D, Hoffmeister KM. Immune cells surveil aberrantly sialylated O-glycans on megakaryocytes to regulate platelet count. Blood. 2021;138:2408–24. [PubMed: 34324649]

[25]. Ju T, Cummings RD. Protein glycosylation: chaperone mutation in TN syndrome. Nature. 2005;437:1252. [PubMed: 16251947]

[26]. Nurden AT, Dupuis D, Pidard D, Kieffer N, Kunicki TJ, Cartron JP. Surface modifications in the platelets of a patient with alpha-N-acetyl-D-galactosamine residues, the TN-syndrome. J Clin Invest. 1982;70:1281–91. [PubMed: 7174794]

[27]. Dunne E, Qi QM, Shaqfeh ES, O'Sullivan JM, Schoen I, Ricco AJ, O'Donnell JS, Kenny D. Blood group alters platelet binding kinetics to von Willebrand factor and consequently platelet function. Blood. 2019;133:1371–7. [PubMed: 30642918]

[28]. Ward SE, O'Sullivan JM, O'Donnell JS. The relationship between ABO blood group, von Willebrand factor, and primary hemostasis. Blood. 2020;136:2864–74. [PubMed: 32785650]

[29]. Zhang XF, Zhang W, Quach ME, Deng W, Li R. Force-regulated refolding of the mechanosensory domain in the platelet glycoprotein Ib-IX complex. Biophys J. 2019;116:1960–9. [PubMed: 31030883]

[30]. Titani K, Takio K, Handa M, Ruggeri ZM. Amino acid sequence of the von Willebrand factor-binding domain of platelet membrane glycoprotein Ib. Proc Natl Acad Sci U S A. 1987;84:5610–4. [PubMed: 3497398]

[31]. King SL, Joshi HJ, Schjoldager KT, Halim A, Madsen TD, Dziegiel MH, Woetmann A, Vakhrushev SY, Wandall HH. Characterizing the O-glycosylation landscape of human plasma, platelets, and endothelial cells. Blood Adv. 2017;1:429–42. [PubMed: 29296958]

[32]. Lewandrowski U, Moebius J, Walter U, Sickmann A. Elucidation of N-glycosylation sites on human platelet proteins: a glycoproteomic approach. Mol Cell Proteom. 2006;5:226–33.

[33]. Tsuji T, Osawa T. The carbohydrate moiety of human platelet glycocalicin: the structures of the major Asn-linked sugar chains. J Biochem. 1987;101:241–9. [PubMed: 3571205]

[34]. Korrel SA, Clemetson KJ, van Halbeek H, Kamerling JP, Sixma JJ, Vliegenthart JF. Identification of a tetrasialylated monofucosylated tetraantennary N-linked carbohydrate chain in human platelet glycocalicin. FEBS Lett. 1988;228:321–6. [PubMed: 3342888]

[35]. Bensing BA, Li L, Yakovenko O, Wong M, Barnard KN, Iverson TM, Lebrilla CB, Parrish CR, Thomas WE, Xiong Y, Sullam PM. Recognition of specific sialoglycan structures by oral streptococci impacts the severity of endocardial infection. PLoS Pathog. 2019;15:e1007896. [PubMed: 31233555]

[36]. Korrel SAM, CLemetson KJ, Halbeek H, Kamerling JP, Sixma J, Vliegenthart JFG. The structure of a fucose-containing O-glycosidic carbohydrate chain of human platelet glycocalicin. Glycoconj J. 1985;2:229–34.

[37]. Hou M, Stockelberg D, Rydberg L, Kutti J, Wadenvik H. Blood group A antigen expression in platelets is prominently associated with glycoprotein Ib and IIb. Evidence for an A1/A2 difference. Transfus Med. 1996;6:51–9. [PubMed: 8696448]

[38]. Santoso S, Kiefel V, Mueller-Eckhardt C. Blood group A and B determinants are expressed on platelet glycoproteins IIa, IIIa, and Ib. Thromb Haemost. 1991;65:196–201. [PubMed: 1711246]

[39]. Curtis BR, Edwards JT, Hessner MJ, Klein JP, Aster RH. Blood group A and B antigens are strongly expressed on platelets of some individuals. Blood. 2000;96:1574–81. [PubMed: 10942408]

[40]. Malaker SA, Pedram K, Ferracane MJ, Bensing BA, Krishnan V, Pett C, Yu J, Woods EC, Kramer JR, Westerlind U, Dorigo O, Bertozzi CR. The mucin-selective protease StcE enables molecular and functional analysis of human cancer-associated mucins. Proc Natl Acad Sci U S A. 2019;116:7278–87. [PubMed: 30910957]

[41]. Rosenbalm KE, Tiemeyer M, Wells L, Aoki K, Zhao P. Glycomics-informed glycoproteomic analysis of site-specific glycosylation for SARS-CoV-2 spike protein. STAR Protoc. 2020;1:100214. [PubMed: 33377107]

[42]. Parker BL, Thaysen-Andersen M, Solis N, Scott NE, Larsen MR, Graham ME, Packer NH, Cordwell SJ. Site-specific glycan-peptide analysis for determination of N-glycoproteome heterogeneity. J Proteome Res. 2013;12:5791–800. [PubMed: 24090084]

[43]. Annarapu GK, Singhal R, Gupta A, Chawla S, Batra H, Seth T, Guchhait P. HbS binding to GP1bα activates platelets in sickle cell disease. PLoS One. 2016;11:e0167899. [PubMed: 27936141]

[44]. Hess D, Schaller J, Rickli EE, Clemetson KJ. Identification of the disulphide bonds in human platelet glycocalicin. Eur J Biochem. 1991;199:389–93. [PubMed: 2070794]

[45]. Aoki K, Perlman M, Lim JM, Cantu R, Wells L, Tiemeyer M. Dynamic developmental elaboration of N-linked glycan complexity in the Drosophila melanogaster embryo. J Biol Chem. 2007;282:9127–42. [PubMed: 17264077]

[46]. Nairn AV, Aoki K, dela Rosa M, Porterfield M, Lim JM, Kulik M, Pierce JM, Wells L, Dalton S, Tiemeyer M, Moremen KW. Regulation of glycan structures in murine embryonic stem cells: combined transcript profiling of glycan-related genes and glycan structural analysis. J Biol Chem. 2012;287:37835–56. [PubMed: 22988249]

[47]. Kumagai T, Katoh T, Nix DB, Tiemeyer M, Aoki K. In-gel β-elimination and aqueous-organic partition for improved O- and sulfoglycomics. Anal Chem. 2013;85:8692–9. [PubMed: 23937624]

[48]. Aoki K, Porterfield M, Lee SS, Dong B, Nguyen K, McGlamry KH, Tiemeyer M. The diversity of O-linked glycans expressed during Drosophila melanogaster development reflects stage- and tissue-specific requirements for cell signaling. J Biol Chem. 2008;283:30385–400. [PubMed: 18725413]

[49]. Mehta N, Porterfield M, Struwe WB, Heiss C, Azadi P, Rudd PM, Tiemeyer M, Aoki K. Mass spectrometric quantification of N-linked glycans by reference to exogenous standards. J Proteome Res. 2016;15:2969–80. [PubMed: 27432553]

[50]. Zhang H, Singh S, Reinhold VN. Congruent strategies for carbohydrate sequencing. 2. FragLib: an MSn spectral library. Anal Chem. 2005;77:6263–70. [PubMed: 16194087]

[51]. Ashline D, Singh S, Hanneman A, Reinhold V. Congruent strategies for carbohydrate sequencing. 1. Mining structural details by MSn. Anal Chem. 2005;77:6250–62. [PubMed: 16194086]

[52]. Varki A, Cummings RD, Aebi M, Packer NH, Seeberger PH, Esko JD, Stanley P, Hart G, Darvill A, Kinoshita T, Prestegard JJ, Schnaar RL, Freeze HH, Marth JD, Bertozzi CR, Etzler ME, Frank M, Vliegenthart JF, Lütteke T, Perez S, et al. Symbol nomenclature for graphical representations of glycans. Glycobiology. 2015;25:1323–4. [PubMed: 26543186]

[53]. Neelamegham S, Aoki-Kinoshita K, Bolton E, Frank M, Lisacek F, Lütteke T, O'Boyle N, Packer NH, Stanley P, Toukach P, Varki A, Woods RJ, Group SD. Updates to the symbol nomenclature for glycans guidelines. Glycobiology. 2019;29:620–4. [PubMed: 31184695]

[54]. Liu Y, McBride R, Stoll M, Palma AS, Silva L, Agravat S, Aoki-Kinoshita KF, Campbell MP, Costello CE, Dell A, Haslam SM, Karlsson NG, Khoo KH, Kolarich D, Novotny MV, Packer NH, Ranzinger R, Rapp E, Rudd PM, Struwe WB, et al. The minimum information required for a glycomics experiment (MIRAGE) project: improving the standards for reporting glycan microarray-based data. Glycobiology. 2017;27:280–4. [PubMed: 27993942]

[55]. Watanabe Y, Aoki-Kinoshita KF, Ishihama Y, Okuda S. GlycoPOST realizes FAIR principles for glycomics mass spectrometry data. Nucleic Acids Res. 2021;49:D1523–8. [PubMed: 33174597]

[56]. Lu L, Riley NM, Shortreed MR, Bertozzi CR, Smith LM. O-pair Search with MetaMorpheus for O-glycopeptide characterization. Nat Methods. 2020;17:1133–8. [PubMed: 33106676]

[57]. Bern M, Kil YJ, Becker C. Byonic: advanced peptide and protein identification software. Curr Protoc Bioinformatics. 2012.

[58]. Perez-Riverol Y, Bai J, Bandla C, García-Seisdedos D, Hewapathirana S, Kamatchinathan S, Kundu DJ, Prakash A, Frericks-Zipper A, Eisenacher M, Walzer M, Wang S, Brazma A, Vizcaíno JA. The PRIDE database resources in 2022: a hub for mass spectrometry-based proteomics evidences. Nucleic Acids Res. 2022;50:D543–52. [PubMed: 34723319]

[59]. Deutsch EW, Bandeira N, Sharma V, Perez-Riverol Y, Carver JJ, Kundu DJ, García-Seisdedos D, Jarnuczak AF, Hewapathirana S, Pullman BS, Wertz J, Sun Z, Kawano S, Okuda S, Watanabe Y, Hermjakob H, MacLean B, MacCoss MJ, Zhu Y, Ishihama Y, et al. The ProteomeXchange consortium in 2020: enabling 'big data' approaches in proteomics. Nucleic Acids Res. 2020;48:D1145–52. [PubMed: 31686107]

[60]. O'Donnell J, Boulton FE, Manning RA, Laffan MA. Amount of H antigen expressed on circulating von Willebrand factor is modified by ABO blood group genotype and is a major determinant of plasma von Willebrand factor antigen levels. Arterioscler Thromb Vasc Biol. 2002;22:335–41. [PubMed: 11834538]

[61]. Gupta R, Brunak S. Prediction of glycosylation across the human proteome and the correlation to protein function. Pac Symp Biocomput. 2002:310–22. [PubMed: 11928486]

[62]. Steentoft C, Vakhrushev SY, Joshi HJ, Kong Y, Vester-Christensen MB, Schjoldager KT, Lavrsen K, Dabelsteen S, Pedersen NB, Marcos-Silva L, Gupta R, Bennett EP, Mandel U, Brunak S, Wandall HH, Levery SB, Clausen H. Precision mapping of the human O-GalNAc glycoproteome through SimpleCell technology. EMBO J. 2013;32:1478–88. [PubMed: 23584533]

[63]. Varki A, Cummings RD, Esko JD, Stanley P, Hart GW, Aebi M, Darvill AG, Kinoshita T, Packer NH, Prestegard JH, Schnaar RL, Seeberger PH. Essentials of glycobiology. 2015.

[64]. Quach ME, Chen W, Li R. Mechanisms of platelet clearance and translation to improve platelet storage. Blood. 2018;131:1512–21. [PubMed: 29475962]

[65]. Franchini M, Favaloro EJ, Targher G, Lippi G. ABO blood group, hypercoagulability, and cardiovascular and cancer risk. Crit Rev Clin Lab Sci. 2012;49:137–49. [PubMed: 22856614]

[66]. He M, Wolpin B, Rexrode K, Manson JE, Rimm E, Hu FB, Qi L. ABO blood group and risk of coronary heart disease in two prospective cohort studies. Arterioscler Thromb Vasc Biol. 2012;32:2314–20. [PubMed: 22895671]

[67]. Etemadi A, Kamangar F, Islami F, Poustchi H, Pourshams A, Brennan P, Boffetta P, Malekzadeh R, Dawsey SM, Abnet CC, Emadi A. Mortality and cancer in relation to ABO blood group phenotypes in the Golestan cohort study. BMC Med. 2015;13:8. [PubMed: 25592833]

[68]. Zhong M, Zhang H, Reilly JP, Chrisitie JD, Ishihara M, Kumagai T, Azadi P, Reilly MP. ABO blood group as a model for platelet glycan modification in arterial thrombosis. Arterioscler Thromb Vasc Biol. 2015;35:1570–8. [PubMed: 26044584]

[69]. Souto JC, Almasy L, Muñiz-Diaz E, Soria JM, Borrell M, Bayén L, Mateo J, Madoz P, Stone W, Blangero J, Fontcuberta J. Functional effects of the ABO locus polymorphism on plasma levels of von Willebrand factor, factor VIII, and activated partial thromboplastin time. Arterioscler Thromb Vasc Biol. 2000;20:2024–8. [PubMed: 10938027]

[70]. Pujol-Moix N, Martinez-Perez A, Sabater-Lleal M, Llobet D, Vilalta N, Hamsten A, Souto JC, Soria JM. Influence of ABO locus on PFA-100 collagen-ADP closure time is not totally dependent on the von Willebrand factor. Results of a GWAS on GAIT-2 project phenotypes. Int J Mol Sci. 2019;20.

[71]. Othman M, Notley C, Lavender FL, White H, Byrne CD, Lillicrap D, O'Shaughnessy DF. Identification and functional characterization of a novel 27-bp deletion in the macroglycopeptide-coding region of the GPIBA gene resulting in platelet-type von Willebrand disease. Blood. 2005;105:4330–6. [PubMed: 15705799]

[72]. Bagdonaite I, Abdurahman S, Mirandola M, Frank M, Narimatsu Y, Vakhrushev SY, Salata C, Mirazimi A, Wandall HH. Isoform-specific O-glycosylation dictates Ebola virus infectivity. 2022.

[73]. Hollenhorst MA, Al-Samkari H, Kuter DJ. Markers of autoimmunity in immune thrombocytopenia: prevalence and prognostic significance. Blood Adv. 2019;3:3515–21. [PubMed: 31730698]

[74]. Zhang N, Curtis BR, Newman PJ. Genetic removal of terminal sialic acid residues from the O-linked glycans adjacent to the HPA-9b polymorphism of platelet membrane glycoprotein IIb improves the binding and detection of HPA-9b patient alloantibodies. Blood. 2021;138:352.

[75]. Goth CK, Halim A, Khetarpal SA, Rader DJ, Clausen H, Schjoldager KT. A systematic study of modulation of ADAM-mediated ectodomain shedding by site-specific O-glycosylation. Proc Natl Acad Sci U S A. 2015;112:14623–8. [PubMed: 26554003]

[76]. Biemann K Appendix 5. Nomenclature for peptide fragment ions (positive ions). Methods Enzymol. 1990;193:886–7. [PubMed: 2074849]

Essentials

- Glycosylation of glycoprotein Ibα is important for platelet function.
- We report a comprehensive and site-specific analysis of human GPIbα glycosylation.
- GPIbα carries sialoglycans, Tn antigen, T antigen, and ABO blood group antigens.
- We experimentally determined 48 O-glycosites and 1 *N*-glycosite by mass spectrometry.

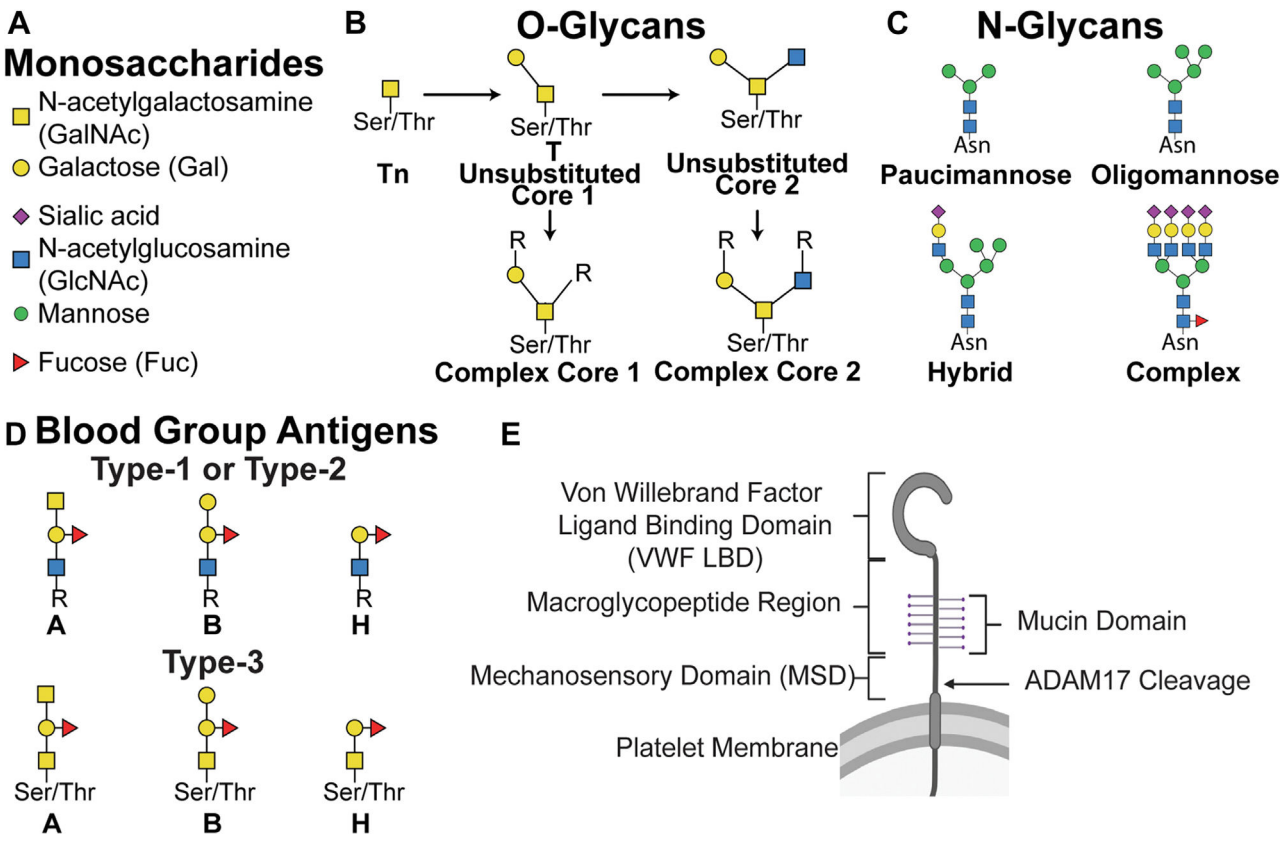

FIGURE 1.

Representative glycan structures. (A) Glycans are complex carbohydrates. Monosaccharides are represented as colored shapes according to Symbol Nomenclature for Glycans standards [52]. (B) O-glycans covalently modify serine (Ser) or threonine (Thr). Important O-glycans include the Tn and T antigens. Complex core 1 or core 2 O-glycans have variable R groups which can include, for example, sialic acid. (C) N-glycans covalently modify asparagine (Asn). Representative glycans are shown from the 4 major classes of N-glycans: paucimannose, oligomannose, hybrid, and complex. (D) ABO blood group is defined by the glycan antigens A, B, and H (H is the antigen found in blood type O individuals). Type-1 and type-2 ABH antigens differ with respect to the linkage between the GlcNAc and Gal (β1,3 for type-1 and β1,4 for type-2). Type-1 ABH antigens are most commonly found as terminal structures on complex O-glycans, and type-2 are most commonly found as terminal structures on *N*-glycans. Type-3 ABH antigens, also known as mucin-associated ABH antigens, are direct modifications of Ser/Thr [63]. (E) Domain organization of GPIbα. GPIbα has an *N*-terminal von Willebrand factor ligand-binding domain (LBD). The C-terminal to this is the macroglycopeptide region, which encompasses the mucin domain. Further C-terminal is the mechanosensory domain (MSD). The ADAM17 protease cleaves intact GPIbα to generate the ectodomain; the cleavage site is within the MSD.

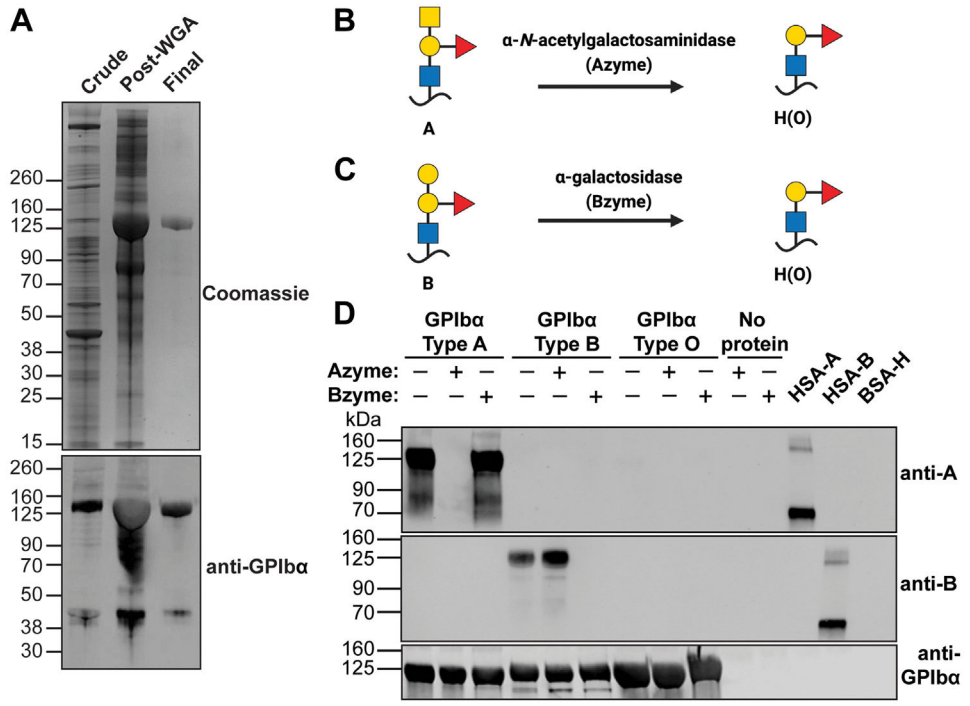

FIGURE 2.

Platelet-derived GPIbα ectodomain carries A and B antigens. (A) GPIbα was purified from human platelets. Samples were analyzed by sodium dodecyl sulfate-polyacrylamide gel electrophoresis with Coomassie total protein stain and by anti-GPIbα Western blot at each step in the purification protocol. The samples analyzed were 1) supernatant following platelet sonication and incubation at 37 °C (crude), 2) after wheat germ agglutinin lectin column (post-wheat germ agglutinin), and 3) after anion exchange chromatography (final). The purified GPIbα appeared as a single band on Coomassie-stained gel. (B) α-*N*-acetyl-galactosaminidase ("Azyme") hydrolysis of the terminal GalNAc of the A antigen to yield the H antigen. (C) α-galactosidase ("Bzyme") hydrolysis of the terminal Gal of the B antigen to yield the H antigen. (D) GPIbα ectodomain purified from human platelets of blood type A, B, or O was untreated or treated with Azyme or Bzyme. The resulting proteins were analyzed by Western blot with anti-A and anti-B antibodies. The following synthetic glycoproteins were used as controls: human serum albumin covalently modified with A antigen, human serum albumin covalently modified with B antigen, and bovine serum albumin covalently modified with the H antigen. Blue square, *N*-acetylglucosamine (GlcNAc); yellow square, N-acetylgalactosamine (GalNAc); yellow circle, Galactose (Gal); red triangle, Fucose (Fuc).

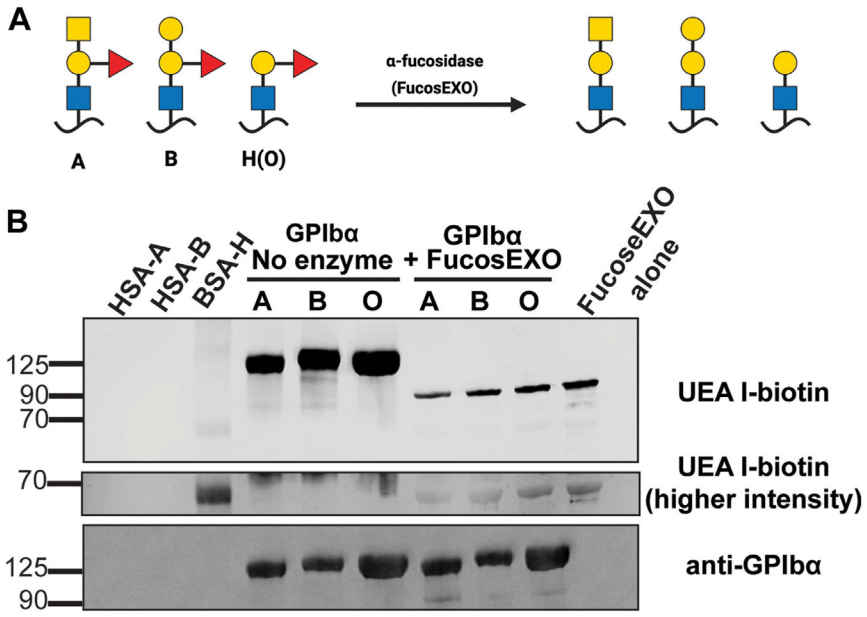

FIGURE 3.

Platelet-derived GPIbα ectodomain carries the H antigen. (A) α-fucosidase (FucosEXO) hydrolysis of ABH antigen fucose to yield defucosylated antigens. (B) GPIbα ectodomain purified from human platelets of blood type A, B, or O was untreated or treated with fucosEXO, and then analyzed by blot with *Ulex europaeus* agglutinin I (UEA-I). UEA-I binds to α-fucosylated glycans and preferentially binds to H antigens. The following synthetic glycoproteins were used as controls: human serum albumin covalently modified with A antigen, human serum albumin covalently modified with B antigen, and bovine serum albumin covalently modified with the H antigen. Blue square, N-acetylglucosamine (GlcNAc); yellow square, N-acetylgalactosamine (GalNAc); yellow circle, Galactose (Gal); red triangle, Fucose (Fuc).

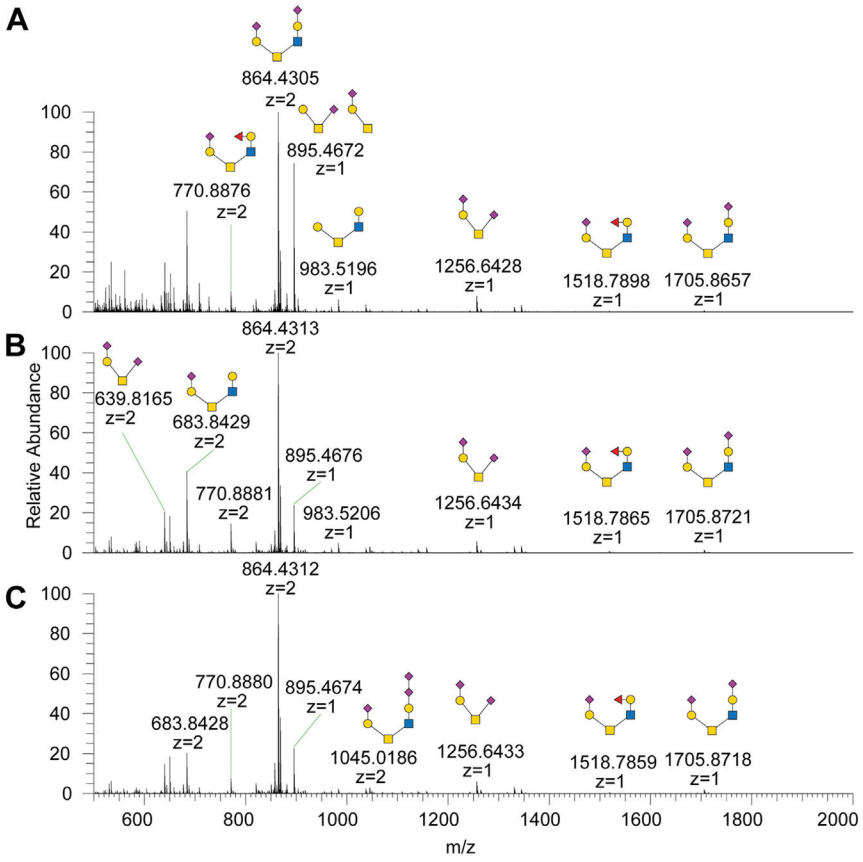

FIGURE 4.

Platelet-derived GPIbα ectodomain O-glycan profiling by MS. O-glycans were released from GPIbα ectodomain purified from human platelets of blood type A, B, or O, respectively. The data shown here are raw MS profiles that include multiply charged ions. GPIbα purified from platelets of blood type: (A) A, (B) B, and (C) O. The structures of isobaric O-glycans were characterized by MS^n analysis. Blue square, N-acetylglucosamine (GlcNAc); yellow square, N-acetylgalactosamine (GalNAc); yellow circle, Galactose (Gal); red triangle, Fucose (Fuc).

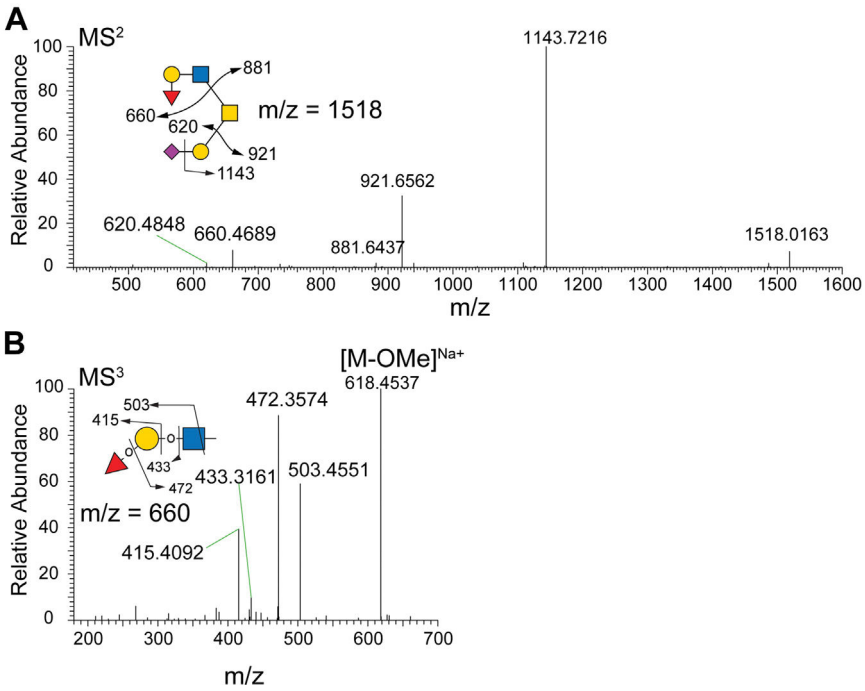

FIGURE 5.

Determination of H antigen on a core 2 O-glycan by MS^n. O-glycomics analysis of type O human platelet-derived GPIbα revealed a glycan with m/z 1518; this is compatible with an extended core 2 O-glycan carrying the H antigen. (A) MS^2 fragmentation of the m/z 1518 O-glycan generated a fragment at m/z 660, compatible with the trisaccharide that defines the H antigen. (B) MS^3 fragmentation of the m/z 660 fragment generated masses consistent with the H antigen (m/z = 503, 472, 433, 415). m/z 618 is the intact glycan Blue square, N-acetylglucosamine (GlcNAc); yellow square, N-acetylgalactosamine (GalNAc); yellow circle, Galactose (Gal); purple diamond, *N*-acetylneuraminic acid (Neu5Ac); red triangle, Fucose (Fuc).

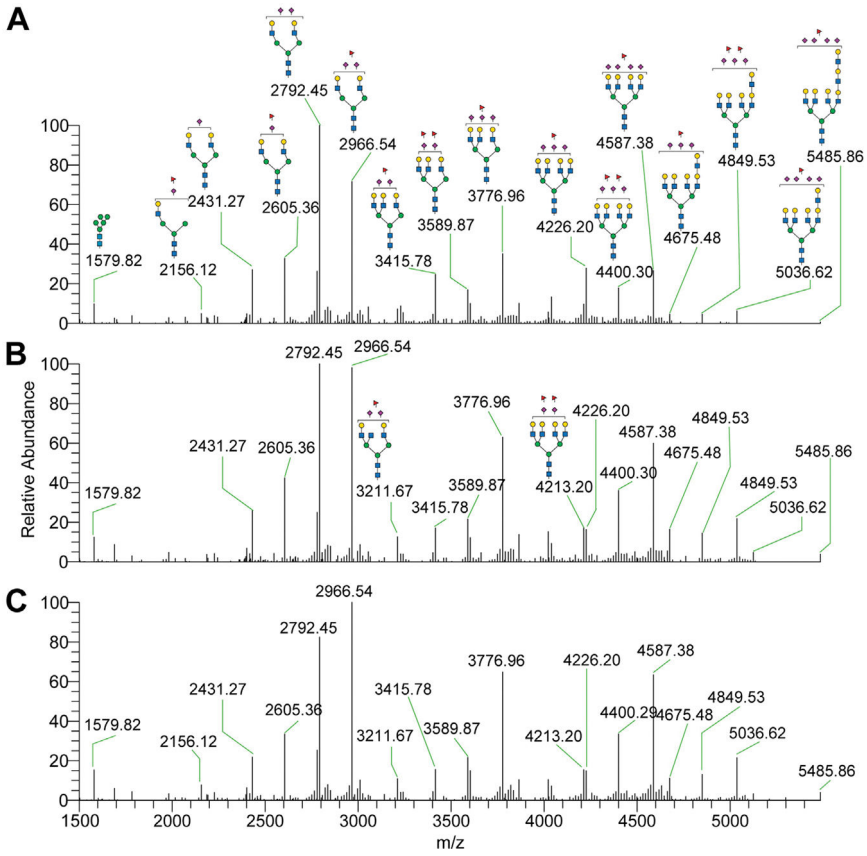

FIGURE 6.

Platelet-derived GPIbα ectodomain N-glycan profiling by MS. N-glycans were released from GPIbα ectodomain purified from human platelets of blood type A, B, or O, respectively. Raw MS profiles were deconvoluted by Xtract software version 2.0. GPIbα purified from platelets of blood type: (A) A, (B) B, and (C) O. We were not always able to unambiguously discriminate between isobaric structures; the graphical representation of the glycan structures indicates the most probable structure(s) based on MS^n analysis and knowledge of typical N-glycan structures and biosynthetic pathways. Many of the detected masses likely represent mixtures of isobaric N-glycans. We were not always able to unambiguously assign 1) the site of attachment of *N*-acetylneuraminic acid, 2) the site of attachment of fucose, and 3) the number of antennae for each N-glycan. Blue square, N-acetylglucosamine (GlcNAc); green circle, Mannose (Man); yellow square, N-acetylgalactosamine (GalNAc); yellow circle, Galactose (Gal); purple diamond, *N*-acetylneuraminic acid (Neu5Ac); red triangle, Fucose (Fuc).

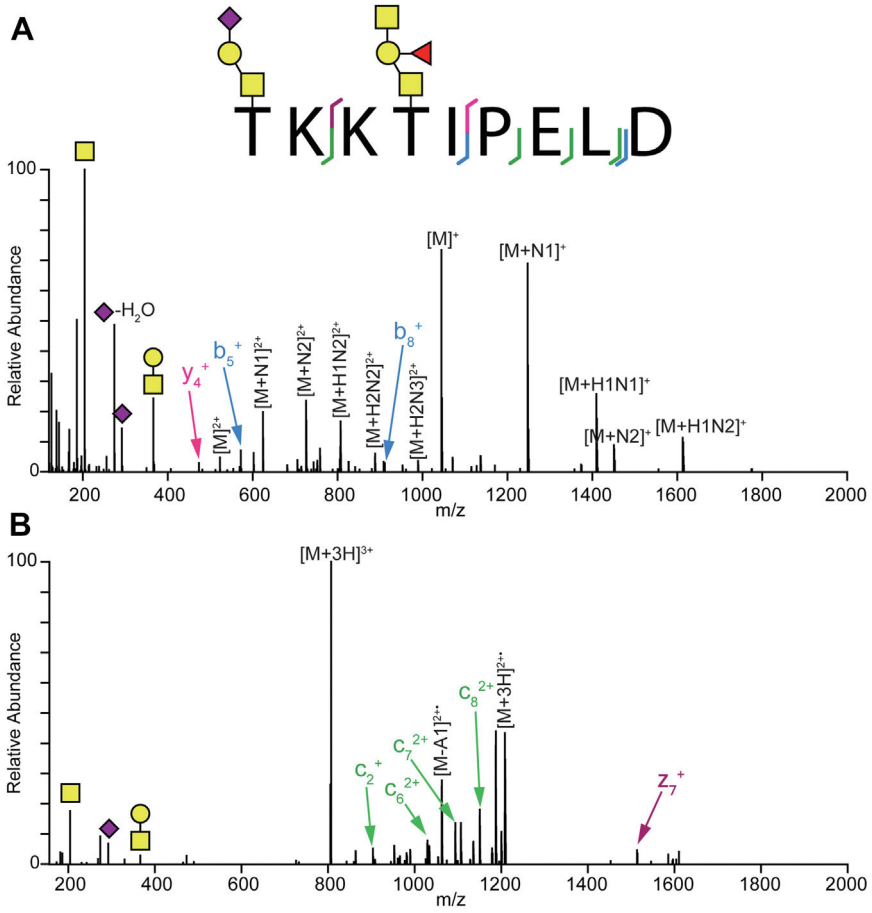

FIGURE 7.

Platelet-derived GPIbα ectodomain glycopeptide analysis by MS. GPIbα purified from human platelets was digested with mucinases, proteases, and/or glycosidases, and then analyzed by MS. The spectra from a representative glycopeptide is shown. This glycopeptide comprises amino acids 491–499 and is glycosylated at T491 and T494. (A) The higher-energy collisional dissociation spectrum revealed *m*/*z* values that matched the non-glycosylated (naked) peptide ($[M+H]^+$, $[M+2H]^{2+}$), and the peptide modified with 1 to 3 monosaccharides (eg, $[M+H1N2]^+$). Several b- and y-ions were detected due to the fragmentation of amide bonds within the naked peptide [76]. The lines on the peptide diagram show where the amide bond cleavages occurred to generate the detected b-ions (blue) and y-ions (magenta); for example, b_5^+ was generated by fragmentation between I495 and P496. (B) The electron transfer dissociation with supplemental activation spectrum revealed *m*/*z* values that matched the intact glycopeptide with the modifications shown ($[M+3H]^{3+}$, $[M+3H]^{2+}$). Several c-ions (green) and z-ions (purple) were detected due to the fragmentation of the N-Cα bonds [76]. The lines on the peptide diagram show where these cleavages occurred to generate the detected c-ions; for example c_2+ was generated by fragmentation between K492 and K493. M, precursor mass; H, hexose; N, *N*-acetylhexosamine; A, *N*-acetylneuraminic acid; F, fucose.

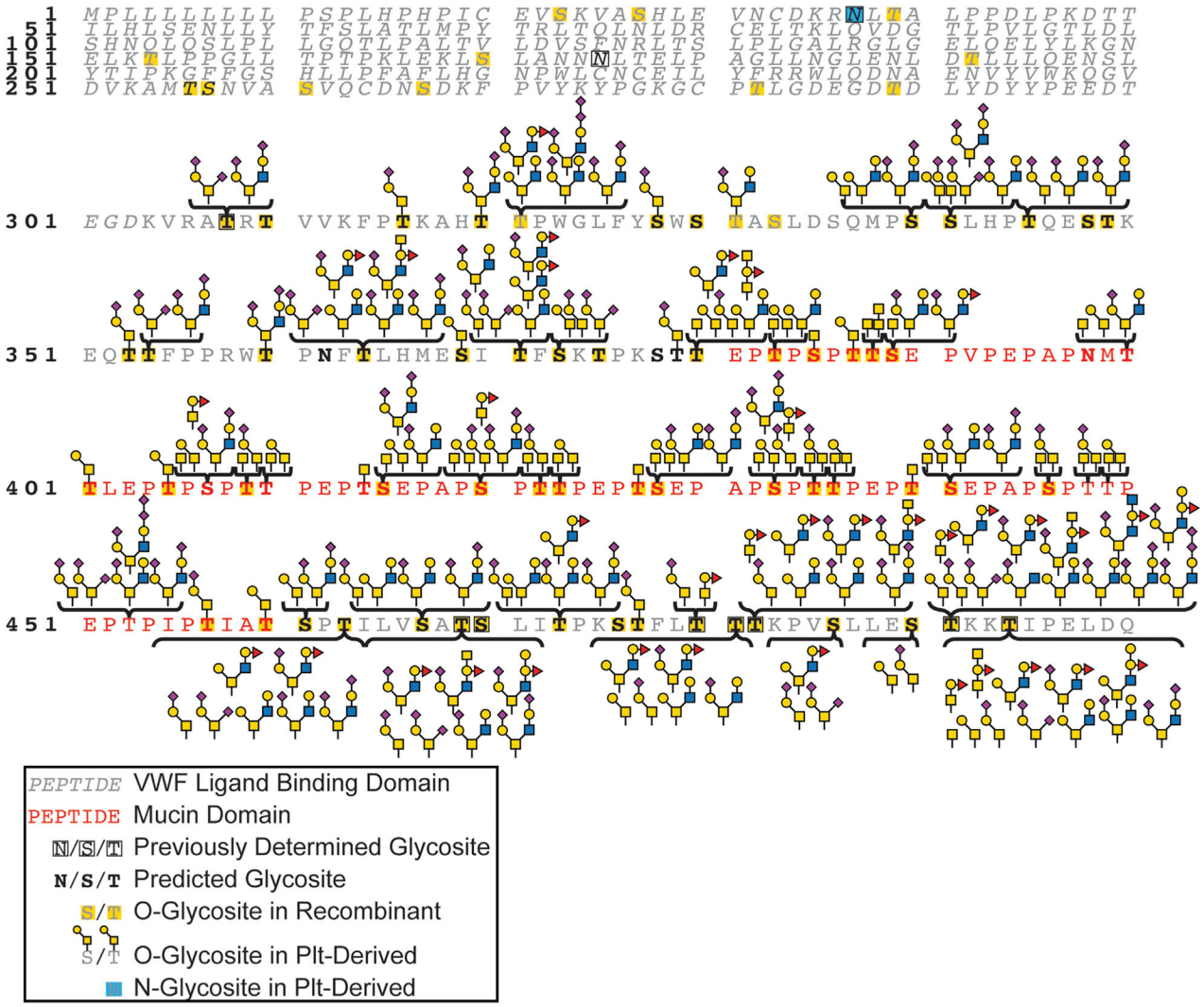

FIGURE 8.

GPIbα ectodomain glycosites and glycan structures determined in this analysis. The GPIbα ectodomain amino acid sequence here is from UniprotKB-P07359.2. The von Willebrand factor ligand-binding domain residues are in italics and mucin domain residues are red. Amino acids that are boxed in black are glycosites that were previously experimentally determined [30–32]. Bolded amino acids are computationally predicted glycosites by NetGlyc. O-glycosites identified in the analysis of the recombinant protein are highlighted yellow. The N-glycosite identified in the analysis of the protein purified from human platelets is highlighted in teal. O-glycosites identified in the analysis of the protein purified from human platelets are indicated with glycans listed above or below the amino acid. The UniprotKB–P07359.2 amino acid sequence includes 3 tandem repeats. The amino acid sequence is identical for 3 stretches of amino acids: 407–419, 420–432, and 433–445. Identified glycosites within these repeats are listed as being present in all 3 repeats, but the sites could not be unambiguously assigned to a particular repeat. VWF, von Willebrand factor; Plt, platelet; Blue square, *N*-acetylglucosamine (GlcNAc); green circle, yellow

circle, yellow square, N-acetylgalactosamine (GalNAc); Galactose (Gal); purple diamond, *N*-acetylneuraminic acid (Neu5Ac); red triangle, Fucose (Fuc).